Miniaturized broadband highly birefringent device with stereo rod-microfiber-air structure

Jun-long Kou,[1,2] Ye Chen,[1] Fei Xu,[1,2,4,*] and Yan-qing Lu[1,3,4]

[1]*National Laboratory of Solid State Microstructures and College of Engineering and Applied Sciences, Nanjing University, Nanjing 210093, China*

[2]*Nanjing University High-Tech Institute at Suzhou, Suzhou 215123, China*

[3]*yqlu@nju.edu.cn*

[4]*Both authors contributed equally to this paper.*

[*]*feixu@nju.edu.cn*

Abstract: A wrapping-on-a-rod technique is presented and demonstrated successfully to realize broadband microfiber-based highly birefringent (Hi-Bi) devices with 3D geometry. By wrapping a circular microfiber (MF) on a Teflon-coated rod (2 mm in diameter), a large and broadband birefringence can be obtained utilizing a rod-microfiber-air (RMA) structure. Wavelength scanning method is used to measure the birefringence of the device. Results show that group birefringence as high as 10^{-3} can be achieved over 400 nm wavelength range. This compact element presents great potential in sensing and communication applications, as well as lab-on-a-rod devices.

OCIS codes: (060.2310) Fiber optics; (060.2420) Fibers, polarization-maintaining; (230.3990) Micro-optical devices.

References and links

1. T. Hosaka, K. Okamoto, T. Miya, Y. Sasaki, and T. Edahiro, "Low-loss single polarization fibres with asymmetrical strain birefringence," Electron. Lett. **17**(15), 530–531 (1981).
2. M. P. Varnham, D. N. Payne, R. D. Birch, and E. J. Tarbox, "Single-polarization operation of highly birefringent bow-tie optical fibres," Electron. Lett. **19**(7), 246–247 (1983).
3. V. Ramaswamy, R. H. Stolen, M. D. Divino, and W. Pleibel, "Birefringence in elliptically clad borosilicate single-mode fibers," Appl. Opt. **18**(24), 4080–4084 (1979).
4. A. Kumar, V. Gupta, and K. Thyagarajan, "Geometrical birefringence of polished and D-shape fibers," Opt. Commun. **61**(3), 195–198 (1987).
5. R. B. Dyott, J. R. Cozens, and D. G. Morris, "Preservation of polarisation in optical-fibre waveguides with elliptical cores," Electron. Lett. **15**(13), 380–382 (1979).
6. X. Chen, M. J. Li, N. Venkataraman, M. T. Gallagher, W. A. Wood, A. M. Crowley, J. P. Carberry, L. A. Zenteno, and K. W. Koch, "Highly birefringent hollow-core photonic bandgap fiber," Opt. Express **12**(16), 3888–3893 (2004).
7. J. L. Kou, M. Ding, J. Feng, Y. Q. Lu, F. Xu, and G. Brambilla, "Microfiber-based Bragg gratings for sensing applications: a review," Sensors (Basel) **12**(7), 8861–8876 (2012).
8. M. Ding, P. Wang, and G. Brambilla, "Fast-response high-temperature microfiber coupler tip thermometer," IEEE Photon. Technol. Lett. **24**(14), 1209–1211 (2012).
9. G. Brambilla, "Optical fibre nanowires and microwires: a review," J. Opt. **12**(4), 043001 (2010).
10. J. L. Kou, J. Feng, L. Ye, F. Xu, and Y. Q. Lu, "Miniaturized fiber taper reflective interferometer for high temperature measurement," Opt. Express **18**(13), 14245–14250 (2010).
11. J. L. Kou, S. J. Qiu, F. Xu, and Y. Q. Lu, "Demonstration of a compact temperature sensor based on first-order Bragg grating in a tapered fiber probe," Opt. Express **19**(19), 18452–18457 (2011).
12. Y. Jung, G. Brambilla, K. Oh, and D. J. Richardson, "Highly birefringent silica microfiber," Opt. Lett. **35**(3), 378–380 (2010).
13. L. Sun, J. Li, Y. Tan, X. Shen, X. Xie, S. Gao, and B. O. Guan, "Miniature highly-birefringent microfiber loop with extremely-high refractive index sensitivity," Opt. Express **20**(9), 10180–10185 (2012).
14. H. Xuan, J. Ju, and W. Jin, "Highly birefringent optical microfibers," Opt. Express **18**(4), 3828–3839 (2010).
15. Y. Jung, G. Brambilla, and D. J. Richardson, "Polarization-maintaining optical microfiber," Opt. Lett. **35**(12), 2034–2036 (2010).
16. G. Wang, P. P. Shum, L. Tong, C. M. Li, and C. Lin, "Polarization effects in microfiber loop and knot resonators," IEEE Photon. Technol. Lett. **22**(8), 586–588 (2010).
17. J. L. Kou, F. Xu, and Y. Q. Lu, "Highly birefringent slot-microfiber," IEEE Photon. Technol. Lett. **23**(15), 1034–1036 (2011).

#176852 - $15.00 USD Received 25 Sep 2012; revised 31 Oct 2012; accepted 14 Nov 2012; published 7 Dec 2012

18. S. C. Rashleigh and R. Ulrich, "High birefringence in tension-coiled single-mode fibers," Opt. Lett. **5**(8), 354–356 (1980).
19. Q. Bao, H. Zhang, B. Wang, Z. Ni, C. H. Y. X. Lim, Y. Wang, D. Y. Tang, and K. P. Loh, "Broadband graphene polarizer," Nat. Photonics **5**(7), 411–415 (2011).
20. J. L. Kou, Z. D. Huang, G. Zhu, F. Xu, and Y. Q. Lu, "Wave guiding properties and sensitivity of D-shaped optical fiber microwire devices," Appl. Phys. B **102**(3), 615–619 (2011).
21. O. Frazão, J. M. Baptista, and J. L. Santos, "Recent advances in high-birefringence fiber loop mirror sensors," Sensors (Basel Switzerland) **7**(11), 2970–2983 (2007).
22. R. Ulrich, S. C. Rashleigh, and W. Eickhoff, "Bending-induced birefringence in single-mode fibers," Opt. Lett. **5**(6), 273–275 (1980).

1. Introduction

Maintaining the polarization state of transmission is of great importance in some systems where random mode coupling of the propagating signal can lead to serious deterioration in system reliability and performance. To overcome this problem, researchers have developed highly birefringent (Hi-Bi) fibers. Conventionally, the internal birefringence of Hi-Bi fibers can be produced by introducing stress applying parts around the fiber core (e.g., commercial PANDA [1], Bow-Tie fibers [2] and internal elliptical cladding fiber [3]) or by geometrical effect of the core (e.g., D-shaped fiber [4] and elliptical core fiber [5]). All these optical fibers support two orthogonally polarized modes and the birefringence is on the order of 10^{-4} - 10^{-5}. Recently, Hi-Bi photonic crystal fibers (PCFs) have also been fabricated [6]. However, all these bulky 125-um-diameter fibers are not suitable for integrating in future micro/nano-photonics. Moreover, the fabrication cost for Hi-Bi PCFs remains a serious problem.

On the other hand, following the ever-growing development of micro/nano-photonics, microfibers (MFs) are of great interest for researchers because of their low loss, large evanescent fields, strong confinement, configurability, and robustness. They have found potential applications in a wide range of fields from telecommunications to sensors, and lasers [7–17]. Among them, Hi-Bi MFs have been proposed or demonstrated exploiting different structures, such as flat fiber with rectangle cross section [12, 13], MF with elliptical cross section [14], MF drawn from commercial PANDA fiber [15] and MF with a slot inside [17].

In this paper, we present a simple and effective wrapping-on-a–rod technique for the fabrication of miniaturized compact broadband MF Hi-Bi devices. Without complex and expensive micromachining facility, MF is drawn from standard single-mode fiber and then wrapped on a low-index rod. We both theoretically predict and experimentally demonstrate a MF-based Hi-Bi device by such a technique utilizing a rod-microfiber-air (RMA) structure. The device with compact 3D geometry shows a large birefringence ($> 10^{-3}$) over 400 nm bandwidth. This compact device presents great potential in sensing and communication applications, as well as lab-on-a-rod devices.

2. Schematic model and theoretical analysis

We first numerically investigate the structure by employing finite element method (FEM). A schematic model in the black dashed box of Fig. 1 is used to study the properties of the stereo RMA structure, which can be obtained by wrapping a circular MF on a rod pre-coated with low-index polymer, such as Teflon used here. The rod only acts as a supporting element which can be any kind of material (polymethyl methacrylate, i.e. PMMA in our experiment) as long as the surface is smooth. Because the thickness of the Teflon film is tens of micrometers, little field will penetrate into the PMMA rod which will be neglected in our calculation. The blue, pink and yellow part in Fig. 1 is the MF, Teflon and supporting rod, respectively. Different coils of the MF are kept away from each other in order to prevent mutual field coupling. If adjacent coils are close enough, a microfiber coil/loop/knot resonator can be realized where the polarization-related coupling effect in the coupling region has to be considered [16]. The rod is 2 mm in diameter which is much larger than the diameter of the MF (~1 - 3 μm). And, as a result, the bending-induced birefringence is not taken into consideration in our cases [18].

#176852 - $15.00 USD Received 25 Sep 2012; revised 31 Oct 2012; accepted 14 Nov 2012; published 7 Dec 2012

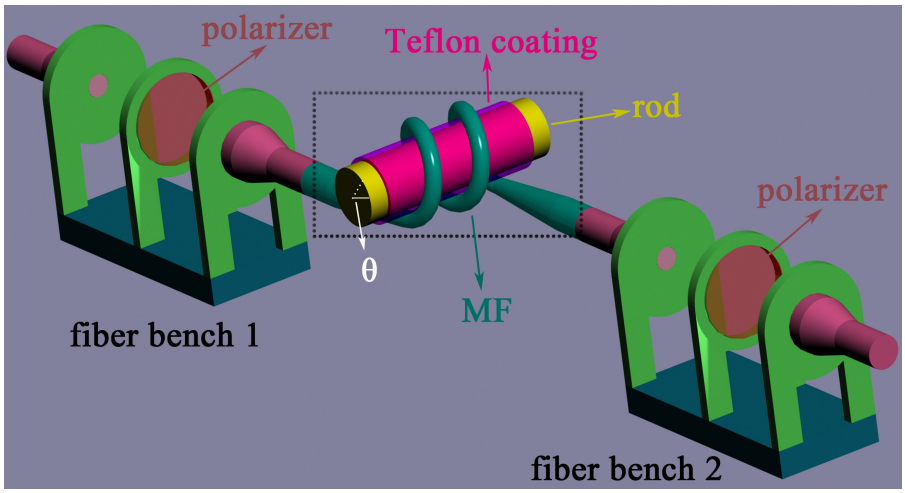

Fig. 1. Experimental setup and schematic of the proposed structure (the black dashed box). In side the box, the blue, pink and yellow part is the MF, Teflon coating and supporting rod, respectively. The rod is 2 mm in diameter and the coating is tens of micrometers in thickness.

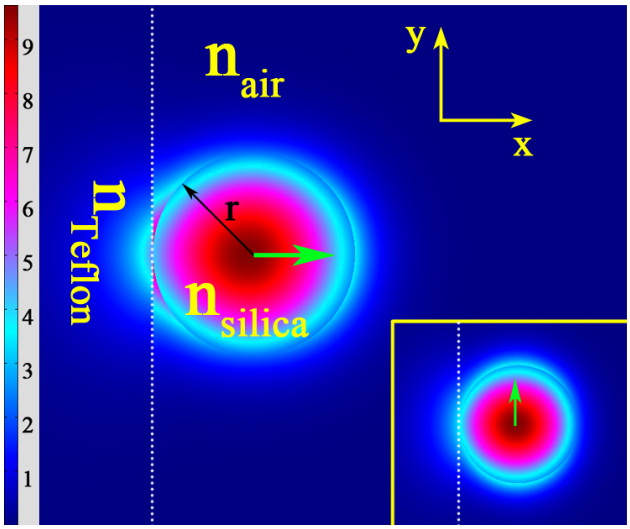

Fig. 2. Cross section and electric field distribution of the RMA structure. Refractive index of different material is labeled in the figure. The green arrow and white dashed line indicates the polarization direction and the boundary between Teflon and air. Inset: electric field distribution of the y-polarized mode. The field is calculated at a wavelength of 1550 nm and r_{MF} = 1 μm.

We numerically investigate the wave guiding properties of the RMA structure. The cross-section of the scheme is shown in Fig. 2. Attributed to the asymmetric refractive index distribution in the two orthogonal directions (x and y in Fig. 2), light with different polarization experiences different effective refractive index, which is similar to that of a D-shaped fiber [19, 20]. And this lays the foundation of the principle employed in this paper. The difference between the effective refractive index is defined as phase birefringence (B_{phase}), result of which is presented in Fig. 3. In our calculation range, it is easily found that a smaller r_{MF} and a longer operation wavelength (λ) results in a larger B_{phase}. As λ decreases, the MF has greater ability to confine the light in the silica region and less evanescent field will penetrate into air or Teflon. It is the same case for increasing r_{MF}, because of which B_{phase} falls. Moreover, in a wide operation wavelength range (1200 - 1650 nm) and MF diameter

#176852 - $15.00 USD Received 25 Sep 2012; revised 31 Oct 2012; accepted 14 Nov 2012; published 7 Dec 2012

range (1.2 - 3 μm), B_{phase} remains larger than 4×10^{-4} which is the typical value for conventional polarization maintaining fibers [21].

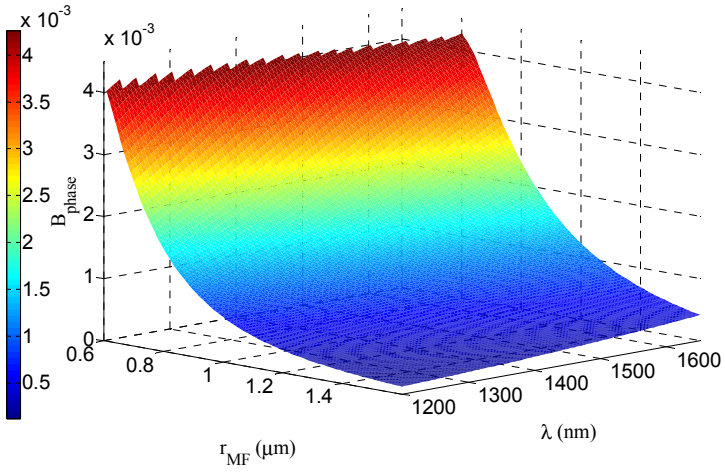

Fig. 3. Calculated B_{phase} of the proposed structure as a function of the radius of the MF and operation wavelength.

3. Experimental fabrication and measurement

First, we use flame-brushing technique to draw the MF from conventional single mode fiber (SMF) which is cost-effective. Prior to the main experiment, we test the polarization properties of the MFs and they show no birefringence. Then, MFs with diameters ranging from 1 μm to 3 μm are wrapped around the PMMA rod (2 mm in diameter) that is pretreated with a coating of Teflon (Teflon® AF 601S1-100-6, a production of DuPont), tens of micrometers in thickness. Due to the high refractive index of PMMA, a thin film of low-index (1.36 @ 1550 nm) Teflon is indispensable in order to prevent the light field from suffering high loss. Because the thickness of the Teflon film is tens of micrometers, little field will penetrate into the PMMA rod which will be neglected in our calculation. To eliminate the field coupling between coils of the MF, distance is kept from coil to coil as shown in the inset of Fig. 4. The total insertion loss of the device is about - 5 dB (blue line in Fig. 4), including loss from the MF with a large evanescent field and bending-induce loss. It can be further minimized by optimizing the tapering process and working environment.

The birefringence of the Hi-Bi RMA samples is measured by wavelength scanning technique as shown in Fig. 1 [12, 14]. Light from a broadband source (NKT, SuperK Versa) is linearly polarized by the first polarizer, exciting two orthogonal polarization modes that propagate through the device and then recombine at the second polarizer, forming interference pattern. The associated transmission spectrum of various samples is recorded by an optical spectrum analyzer (Yokogawa, AQ6370C). The transmission spectrum of our RMA structure can be predicted by

$$T(\lambda) \propto \cos^2\left(\frac{\pi \int B_{phase}(\theta,\lambda) R d\theta}{\lambda}\right) \quad (1)$$

where B_{phase} is a function of the azimuth angle because the radius of the MF taper wrapped around the rod is not uniform and R is the radius of the rod. Experimental results are shown in Fig. 4. As can be seen, large extinction ratio (16 dB - 32 dB) covering 400 nm bandwidth is obtained which indicates excellent polarization maintaining properties. However, noise in the spectrum increases when the wavelength is below ~1300 nm attributed to the fact that at these

#176852 - $15.00 USD Received 25 Sep 2012; revised 31 Oct 2012; accepted 14 Nov 2012; published 7 Dec 2012

wavelengths, the fiber becomes multi-mode. Moreover, according to previous literature, bending-induced birefringence of our scheme is on the order of 10^{-6} which is negligible [22]. In order to confirm this, we also examine the spectrum by immersing the RMA structure in Teflon solution. Results show that birefringence disappears after the asymmetry is broken.

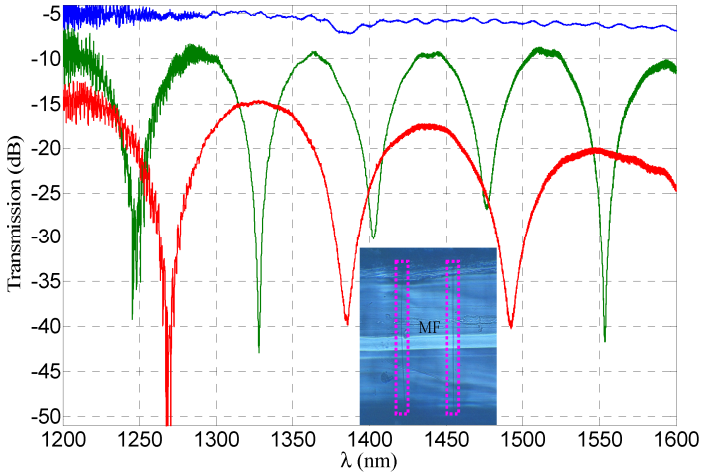

Fig. 4. Measured transmission spectra of the proposed RMA structure. The blue line is the insertion loss of Sample 1. The green and red line is the transmission of two devices with MF of different diameter (green for Sample 1, d_{MF} = 1.5 μm and red for Sample 2, d_{MF} = 1.7 μm). Inset: optical microscopic picture of one sample. The pink boxes indicate two coils of MF. The distance between the coil is ~100 μm.

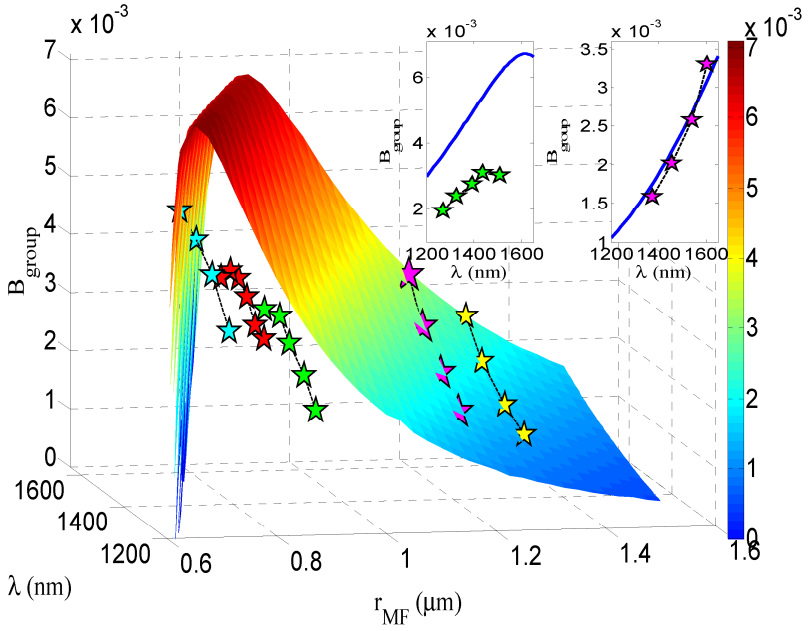

Fig. 5. B_{group} calculated from FEM method (3D mesh) and that from experimental transmission spectrum (solid asterisks with different colors). Inset: 2D illustration of the experimental (solid asterisks with different colors) and theoretical (blue lines) results of two samples with different radius (left for r_{MF} = 0.9 μm and right for r_{MF} = 1.2 μm). The data is extracted form the 3D mesh.

#176852 - $15.00 USD Received 25 Sep 2012; revised 31 Oct 2012; accepted 14 Nov 2012; published 7 Dec 2012

Limited by the length of the MF, our samples contain one or two coils of MF and this results in large free spectrum range (FSR). In addition, the radius of the MF is not uniform in the region that wrapped on the rod. Thus, we can only obtain an average group birefringence (B_{group}) of our RMA samples. The results are calculated by Eq. (2) with experimental data from the spectrum.

$$B_{group}(\lambda, r_{MF}) \approx \frac{\overline{\lambda}^2}{FSR \times L} \tag{2}$$

L is the length of the MF wrapped around the rod. Solid asterisks in Fig. 5 show B_{group} of our samples with different r_{MF} (measured at the thinnest waist of the MF) calculated from the spectrum. It is clear that a large B_{group} ~10^{-3} which is more than one order of magnitude than in conventional Hi-Bi fibers is achieved over the measured range and reaches ~4×10^{-4} at ~1415 nm for one particular sample (red asterisks in Fig. 5). In our measured range, a longer wavelength sees a larger B_{group} when $r_{MF} > 0.9$ μm.

The high birefringence of the RMA structure can also be confirmed by theoretically calculating B_{group}, which is related to B_{phase} by

$$B_{group} = B_{phase} - \lambda \frac{dB_{phase}}{d\lambda} \tag{3}$$

B_{group} exhibits a behavior notably different from B_{phase}. For MF with diameter less than the operation wavelength, B_{group} is small. However, it rises steeply to reach its peak value that is significantly larger than B_{phase}. The reason for this difference is the derivative of B_{phase} with respect to the wavelength, which is large at small MF diameter. After crossing over the peak value, B_{group} decreases at a tendency similar to that of B_{phase}. Comparing the results from the experimental data and that from FEM method, we find that they agree well with each other when $r_{MF} > 1.1$ μm. Although r_{MF} is not uniform and λ is just an average value, in this region, B_{group} changes slowly with respect to λ and r_{MF}. However, it is not the case around the region where B_{group} reaches its peak value. In fact, B_{group} turns out to be a fast-varying function of λ and r_{MF} around this region, especially in the longer wavelength and bigger radius side. Considering that r_{MF} is not uniform along the coil on the rod and that the radius labeled in Fig. 5 is the thinnest measured, the difference between the results from the experiment and that from theory is reasonable. The radius of the MF is directly related to the spread of the evanescent field into the Teflon coating and air which determines the birefringence. Thus, controlling the radius of the MF is a key point in obtaining a large birefringence.

4. Conclusions

In this paper, we both theoretically exploit and experimentally realize a new kind MF-based Hi-Bi device which incorporates wrapping a MF around a rod that is pretreated with Teflon coating. This compact and cost-effective device could operate over a broad bandwidth with birefringence higher than 10^{-3}. The fabrication technique of wrapping-on-a-rod is effective and low-cost. More novel and compact lab-on-a-rod devices can be explored by flexible design of rod material or coil profile. Our investigation of it would put insight into the application of MF in future fiber communication, sensing and micro/nano-photonics.

Acknowledgments

This work is supported by National 973 program under contract No. 2012CB921803 and 2011CBA00205, NSFC program No. 11074117 and 60977039, Natural Science Foundation of Jiangsu Province of China under contract No. BK2010247. The authors also acknowledge the support from PAPD and the Fundamental Research Funds for the Central Universities.

#176852 - $15.00 USD Received 25 Sep 2012; revised 31 Oct 2012; accepted 14 Nov 2012; published 7 Dec 2012